

DERIVING MICROPHYSICAL PARAMETERS OF SNOW WITH A VERTICALLY POINTING DOPPLER RADAR

E. Moreau^{*1}, J. Testud¹, and I. Zawadzki²

¹NOVIMET, Velizy, France

²Marshall Radar Observatory, Mc Gill University, Montréal, Québec, Canada

1. INTRODUCTION

Large uncertainties remain on the retrieval of the snow microphysical characteristics by radar due to the natural variability of the drop size distribution and of the bulk density of ice particles. In this context, a Z-R relationship may not represent this natural variability.

In this paper, the Snow Profiling Algorithm (SPA) is proposed in order to derive snow microphysical characteristics from vertical profile of reflectivity (Z) as input. SPA models the aggregation, which is a major process in the stratiform precipitation.

Retrieval of SPA using X-band radar data from McGill University (Montreal, Canada) are presented and compared with co-located drop size distribution measurements. The Doppler measurement is used to validate the retrieval profiles and in particular the bulk density hypothesis.

2. SNOW PROFILING ALGORITHM (SPA)

This algorithm is appropriate in conditions of stratiform precipitation. The stratiform precipitation process implies that the pristine ice crystals are initiated at high altitude (i.e. at very low temperature), where many ice nuclei are activated. Ice crystals then grow during their sedimentation through three main processes: water vapor deposition, riming, and aggregation. Among these three processes, only aggregation changes the particle concentration.

SPA is based on a simple aggregation model that describes the evolution in altitude of the particle concentration.

As a profiling algorithm, SPA inverts the vertical profile of Z (in ice) to deliver the corresponding profiles of various physical parameters of interest: mean particle mass diameter D_m , particle concentration n_T , intercept parameter N_0 , ice water content IWC and melted precipitation rate R.

The kernel of SPA lies on the fact that n_T change results from collisions between particles. Such collisions occur because of the differential sedimentation velocity between particles, due to the variability of particle diameters. In this model, the terminal velocity of each diameter is related to its density through the formulation of Mitchell (1996). Integrating such differential velocity in the sample volume gives rise to the collision frequency.

Because aggregation may result from a proportion of collisions only, an efficiency coefficient depending of the altitude is applied.

The input of the model is the profile of measured reflectivity factor Z. This information is ingested in the model through a (Z/N_0) - D_m relationship.

Moreover, additional assumptions are required: the number of ice nuclei at the top of the cloud which temperature dependent, an exponential particle size distribution (Delanoë et al., 2004) and the density particle size relationship:

$$\rho(D) = \rho_{ice} \left(\frac{D}{D_{min}} \right)^\gamma \quad (1)$$

for $D > D_{min}$, and $\rho = \rho_{ice}$ otherwise.

3. DOPPLER CONSIDERATIONS

The Doppler velocity measured by a vertically pointing radar V_D is the sum of the reflectivity-weighted particle vertical velocity V_Z and of the vertical air velocity V_a :

$$V_D = V_a + V_Z \quad (2)$$

The reflectivity weighted particle vertical velocity V_Z is given by:

$$V_Z = \frac{\int V(D) N(D) \sigma_r(D) dD}{\int N(D) \sigma_r(D) dD} \quad (3)$$

where σ_r is the backscattering cross-section.

* Corresponding author address: Emmanuel Moreau, NOVIMET, 10-12 av. de l'Europe, 78140 Velizy, France; e-mail: emmanuel.moreau@novimet.com

Neglecting the vertical air velocity (for stratiform cases), the Doppler velocity may give useful information about the density of the ice particles along the vertical profiles, throughout the formulation of Mitchell (1996).

3. OBSERVATIONS

By October 25, 2002, a stratiform precipitation was sampled by an X-band vertically pointing Doppler radar, at McGill, Canada. The measuring reflectivity and Doppler velocity are presented in figures 1 and 2. The bright band is easily identified by the increase of the reflectivity around 1km height. In the snow layer, the reflectivity increase from 6.2km height down to the top of the bright band reaching values around 30dB. Two situations can be identified

Region I, around 13hr, characterized by high Z and V_D near the freezing level and surface rainfall rates around 5 mm.h^{-1} .

Region II, around 16hr, characterized by a lower V_D and surface rainfall rates less than 1 mm.h^{-1} .

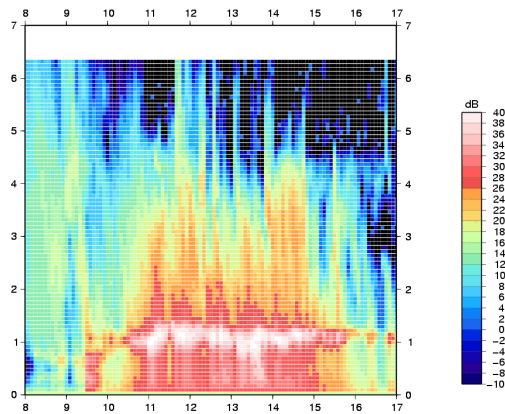


Figure 1: Height [m]-Time [min] reflectivity, VPR, 25/10/2002, McGill, Canada.

4. DISCUSSION

For comparison, data obtained from a collocated POSS (Precipitation Occurrence Sensor System) have been used, providing drop size distributions for rain precipitation at the ground level. Details of the treatment are described by Shepard (1990).

Results of SPA are presented in figures 3 and 4, showing the time evolution at the top of the bright band of D_m , N_0^* and R parameters using two different density laws; setting D_{min} to 0.08mm (*density I*) and 0.14mm (*density II*) respectively (γ is set to -1).

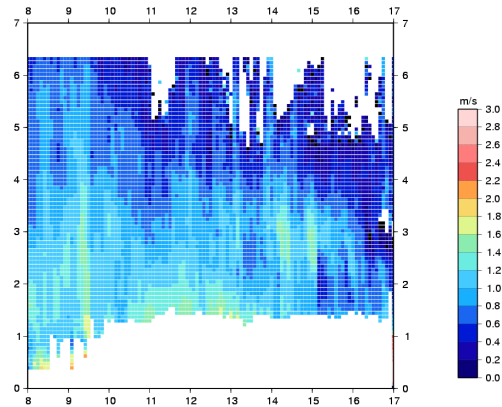


Figure 2: Height [m]-Time [min] Doppler velocity in the snow layers, VPR, 25/10/2002, McGill, Canada.

Large differences can be observed between the two density hypothesis in terms of D_m and N_0^* . The rainfall rates remain very similar. Setting D_{min} to 0.08mm is equivalent to considering low density particles. In region I, this hypothesis does not seem correct, leading to larger D_m compared to the one measured by the POSS instrument. In opposite, the second density assumption gives results in much better agreement with POSS measurements.

Identifying the best density assumptions may be achieved by comparing the measured and retrieved V_D (figures 5 and 6)

In region I:

- *density I* produces closed V_D in average over the whole vertical profile, too high at the top of the profile and too low at the freezing level.
- *density II* produces closed V_D near the freezing level only.

From this comparison we may suggest that the *density I* be correct up to 500m above the BB and *density II* below.

In region II:

- *density II* is clearly in better agreement than *density I* along the whole vertical profile. Nevertheless, both density models give very similar results with small D_m corresponding to very low rainfall rates ($< 1 \text{ mm.h}^{-1}$).

7. ACKNOWLEDGEMENTS

We wish to thank Dr. Gyu Won Lee from McGill University who kindly provided the radar data as well as the POSS data.

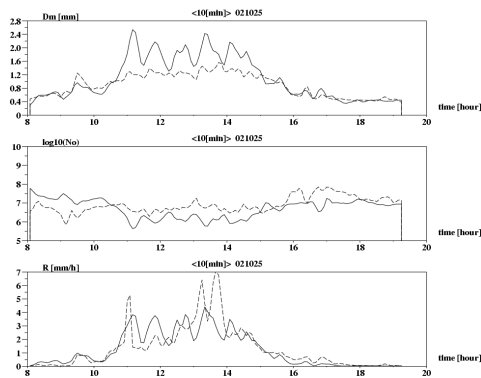


Figure 3: Time evolution at the top of the bright band of D_m , N_0 and RR parameters retrieved by SPA with *density I* (solid lines) and collocated measured at the surface from the POSS instrument.

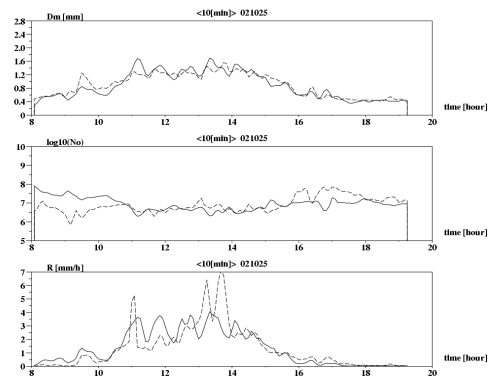


Figure 4: Same as previous but with density II.

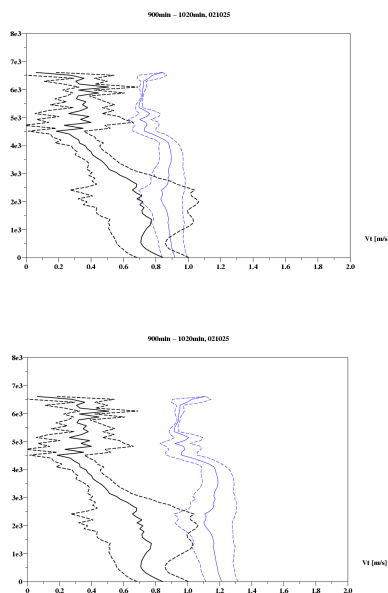


Figure 5: Vertical profile of Doppler velocity retrieved by SPA (blue) and measured by X-band radar (black) averaged between 15h and 17h (region II). Dotted lines stand for \pm one standard deviation. Using density I (top panel) and density II (bottom panel). 25/10/2002, McGill, Canada.

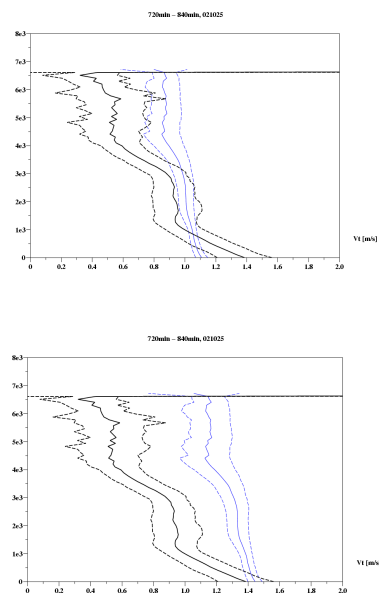


Figure 6: Same as previous, but averaged between 12h and 14h (region I).

8. REFERENCES

Mitchell D.L., 1996: Use of mass and area dimensional power laws for determining precipitation particle terminal velocities. *J. Atmos. Sci.*, 51, 797-816.

Sheppard B.E., 1990: Measurement of raindrop size distributions using a small Doppler radar, *J. Atmos. Oceanic Technol.*, 7, 255-268.

Delanoë J., A. Protat, J. Testud and D. Bouniol, 2004: Statistical properties of normalized ice particle size distributions from in-situ microphysical measurements. Part I: Stability of the shape of the normalized distribution. *J. Appl. Meteor.*, *accepted*.